JOURNAL OF MATERIALS SCIENCE 28 (1993) 6427–6432

The influence of base metal grain size on isothermal solidification during transient liquid-phase brazing of nickel

K. SAIDA*, Y. ZHOU, T. H. NORTH
Department of Metallurgy and Materials Science, University of Toronto, Ontario, Canada

The influence of base metal grain size on isothermal solidification during transient liquid-phase brazing with Ni–11 wt% P filler metal has been investigated. Single-crystal, coarse-grained and fine-grained nickel base metal were brazed at 1150 °C for various holding times. The eutectic width decreased linearly with the square-root of the brazing time in single-crystal, coarse-grained and fine-grained nickel base metals. The completion time for isothermal solidification decreased in the order single-crystal, coarse-grained and fine-grained nickel base metal. The difference in isothermal solidification rates produced when brazing the different base metals is explained qualitatively by the influence of base metal grain boundaries on the apparent mean diffusion coefficient of phosphorus in solid nickel.

1. Introduction

The transient liquid-phase (TLP) brazing operation comprises three sequential processes, namely, base metal dissolution, isothermal solidification at the brazing temperature and homogenization following complete solidification of the joint. Isothermal solidification is the most important and characteristic phenomenon which occurs during TLP brazing and consequently much research has been carried out on this aspect of the brazing process.

The detailed effects which occur during TLP brazing have recently been elucidated [1–3], and modelled [4, 5]. Nakagawa *et al.* [6] employed one-dimensional finite difference modelling to analyse base metal dissolution behavior and isothermal solidification during TLP brazing of Ni-200 base metal, and emphasized the importance of filler metal thickness, and of heating rate between the filler metal melting temperature and the brazing temperature, on the dissolution process. North *et al.* [7] compared the experimental completion times produced during isothermal solidification with calculated values and suggested that the substantial discrepancy between these results was explained by the influence of base metal grain size on movement of the solid–liquid interface during TLP-brazing. In this connection, Tuah-Poku *et al.* [8] also suggested that liquid penetration at grain-boundary regions explained the marked difference between their calculated and experimental completion times for isothermal solidification during TLP brazing of silver using copper filler metal.

Kokawa *et al.* [9] examined the solid–liquid interface in detail using scanning electron microscopy and the electron channelling pattern (ECP) technique and observed that the liquid penetration depth depended on the amount of misorientation at base metal grain boundaries (liquid penetration was greatest at high-angle grain boundaries). Ikeuchi *et al.* [10] analysed liquid penetration at grain boundaries using two-dimensional modelling and found that it depended on a combination of factors, namely, high solute diffusivity at grain boundaries, and the interfacial energy balance between the grain boundary and the solid–liquid interface.

Although the TLP brazing process has been extensively examined, little research has evaluated the influence of base metal grain boundaries on the rate of completion of the isothermal solidification process. The paper investigated present work on the effect of base metal grain size on movement of the solid–liquid interface, and on the time required for completion of isothermal solidification.

2. Experimental procedure

2.1. Materials

The base metal was nickel which had different grain sizes, namely single-crystal, coarse-grained and fine-grained material. The nominal purities of the nickel base metal are shown in Table I. In the single-crystal material, the (1 0 0) orientation of the face-centred-cubic lattice was always aligned perpendicular to the joint interface. The coarse-grained nickel was Ohno-cast [11, 12] and had a grain size of ~3.5 mm. The fine-grained base material had an average grain size of 200 μm. The single-crystal and fine-grained base materials were employed in the as-received condition, while the coarse-grained, Ohno-cast base material was

* *Permanent address*: Department of Welding and Production Engineering, Osaka University, Osaka, Japan.

0022–2461

TABLE I Nickel base metals and filler metal used

Material	Purity (wt %)	Grain size (mm)	Dimensions (mm)		Remarks
			Diameter	Thickness	
Ni					
Single-crystal	99.999	(12.5)	12	3	(1 0 0) orientation, as-received
Coarse-grained	99.99	3.5	12	5	Ohno-cast Ni, 1150 °C × 24 h
Fine-grained	99.5	0.20	12	5	As-received
Filler metal	Ni–11 wt %P		10		Thickness 25 μm

annealed at 1150 °C for 24 h in vacuum prior to brazing.

The test specimen dimensions were 12 mm diameter × 3 mm thick (for the single-crystal material) and 12 mm diameter × 5 mm thick (for the coarse-grained and fine-grained base metals). 25 μm thick Ni–11 wt % P brazing filler metal was employed throughout testing.

2.2. Experimental procedure

The faying surfaces of the nickel samples were polished using 1200 grade emery paper to remove the deformed surface layer produced by specimen machining and to make the surfaces smoother. All test specimens were then ultrasonically cleaned with acetone immediately prior to spot welding. The filler metal was inserted at the joint interface and the spot welds, together with the nickel clamping fixture, maintained a constant gap width at the joint interface. The two spot welds present at the joint interface promoted intimate contact between the filler and base materials (see Fig. 1). Escape of liquid filler metal during the brazing operation was prevented by painting alumina-based stop-off material at the joint periphery. All brazing tests were completed in a vertically-aligned Lindberg glow-bar furnace (see Fig. 2). The brazing furnace was configured so that an individual test specimen could be quenched into an oil bath while under vacuum. Because the distribution of temperature along the length of the Lindberg furnace was known, the test samples were raised to a specific location (temperature zone) in the furnace. Using this experimental arrangement, the heating time between the filler metal melting temperature (880 °C) and the brazing temperature (1150 °C) was minimized. In this study, the heating rate between the filler metal melting point and the brazing temperature was 2.5 °C s^{-1}. After a given holding period at the brazing temperature, the test specimen was dropped into the oil-quenching bath.

The brazing temperature was 1150 °C throughout and this temperature was maintained within ± 5 °C

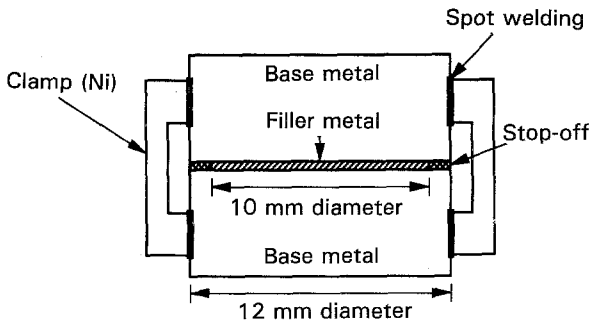

Figure 1 Configuration of the TLP brazing assembly.

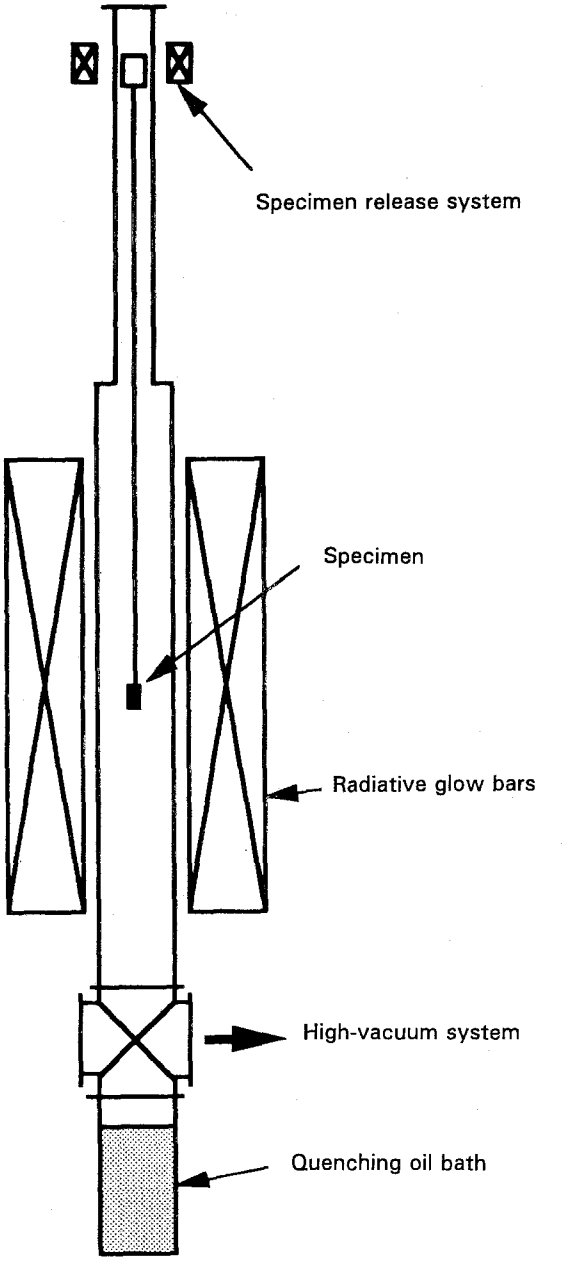

Figure 2 Schematic drawing of the vacuum brazing furnace with the oil-quenching facility.

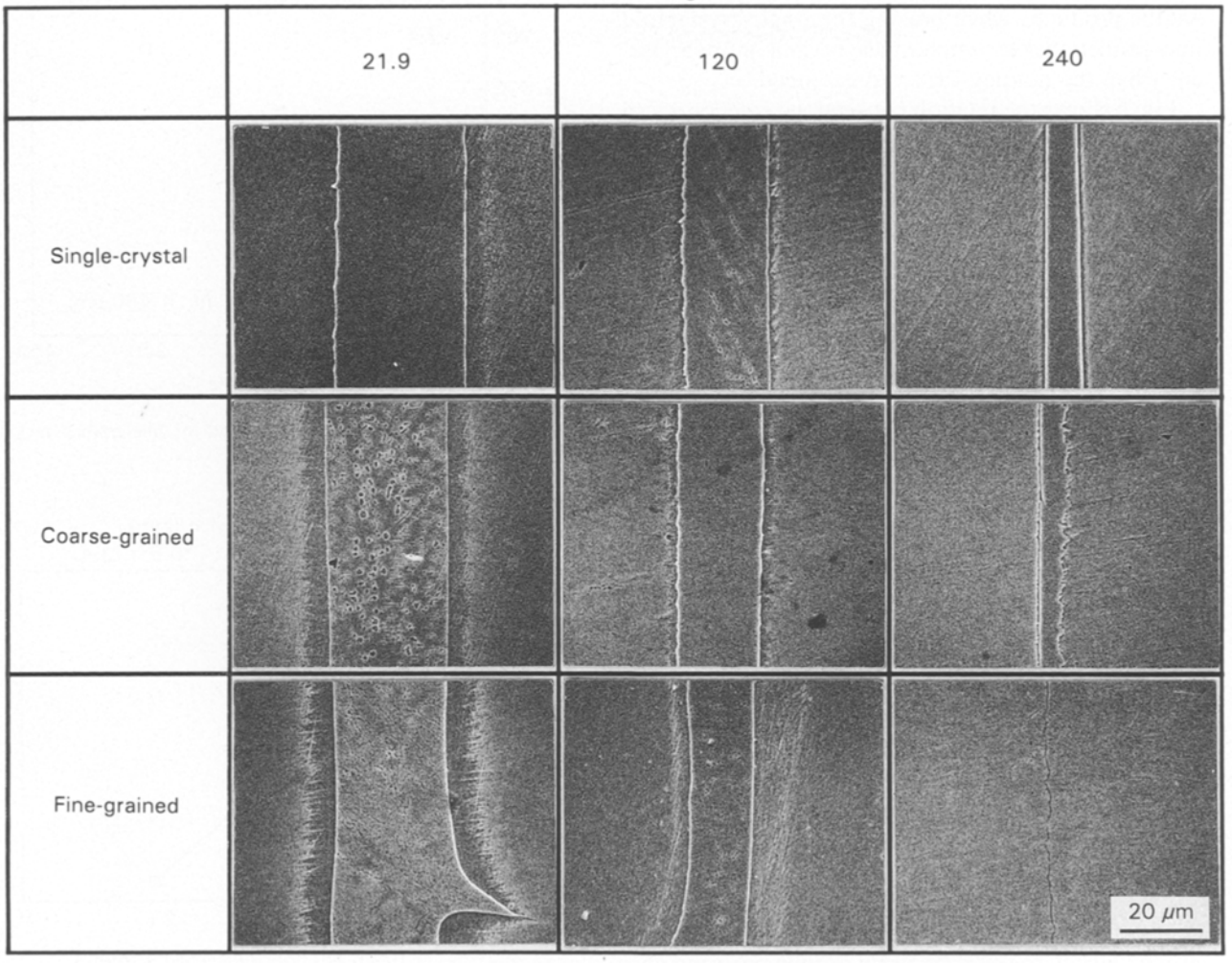

Figure 3 Brazed layer microstructures produced at different holding times (for nickel base metals having different grain sizes).

during the holding period. The vacuum during brazing was maintained at 10^{-5} torr (1 torr = 133.322 Pa).

2.3. Metallography

All test samples were examined using a combination of optical and scanning electron microscopy (SEM). The test samples were etched as follows:

(i) for observing the brazed layer: in a solution of 1 part concentrated nitric acid/1 part glacial acetic acid;

(ii) during grain-size measurement: in a solution of 1 part concentrated nitric acid/2 parts concentrated hydrochloric acid/3 parts glycerine.

The average width of the eutectic phase in the brazed layer was measured by evaluating the cross-sectional area of the eutectic phase at × 500 magnification. The eutectic width was evaluated over a distance of 5 mm at the mid-section of the brazed test specimens, and the base metal grain size was measured immediately adjacent to the brazed layer over the whole length of the joint interface.

3. Results

3.1. Change in eutectic width during isothermal solidification

The effect of base metal grain size on the rate of isothermal solidification during TLP brazing was evaluated by comparing the results produced using single-crystal, coarse-grained and fine-grained nickel base metals. Fig. 3 compares the oil-quenched brazed layer microstructures produced with the different base metals (for brazing times of 8 min (21.9 $s^{1/2}$), 4 h (120 $s^{1/2}$) and 16 h (240 $s^{1/2}$). The eutectic widths in the fine-grained base metal were much narrower than those produced using the single-crystal and coarse-grained nickel base metals (for equivalent holding

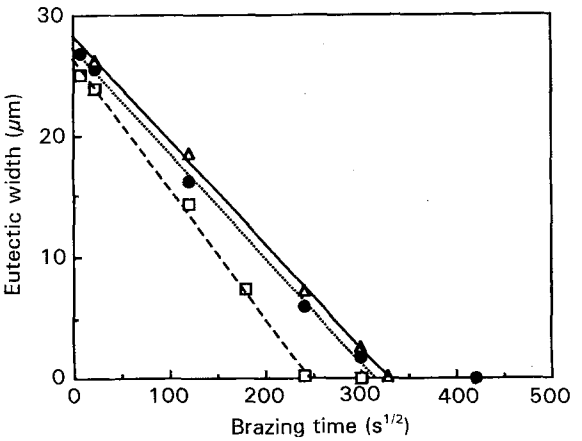

Figure 4 Relation between the eutectic width and the square-root of the holding time for base metals with different grain sizes: (□) fine-grained, (●) coarse-grained, (△) single-crystal.

times at 1150 °C). Also, the difference in eutectic widths produced when brazing the single-crystal and fine-grained nickel samples base became more apparent when the holding time was extended.

Fig. 4 shows the relation between the eutectic width and holding time at the brazing temperature for the different nickel base metals. The eutectic widths decreased linearly with the square-root of brazing time for all base metals. The rate of isothermal solidification of the single-crystal and coarse-grained nickel samples were very similar, while that in fine-grained nickel was much faster. The eutectic widths at the beginning of the isothermal solidification process were slightly decreased in the order single-crystal, coarse-grained and fine-grained nickel base metals.

3.2. Grain growth in the base metal during TLP brazing

The effect of holding time at the brazing temperature on grain growth in the different nickel base metals was investigated as a preliminary step before considering the influence of grain boundaries on the rate of isothermal solidification. Fig. 5 shows the effect of holding time at the brazing temperature on the grain size of coarse-grained nickel base metal. The initial grain size prior to the TLP brazing was that produced following annealing at 1150 °C for 24 h and, as expected, little variation in grain size occurred during the TLP brazing operation. The average grain size throughout the isothermal solidification process was 3.4 mm. Fig. 6 shows the grain size/holding time relation for fine-grained nickel. In this case, grain growth occurred and the mean grain size during isothermal solidification was 480 μm.

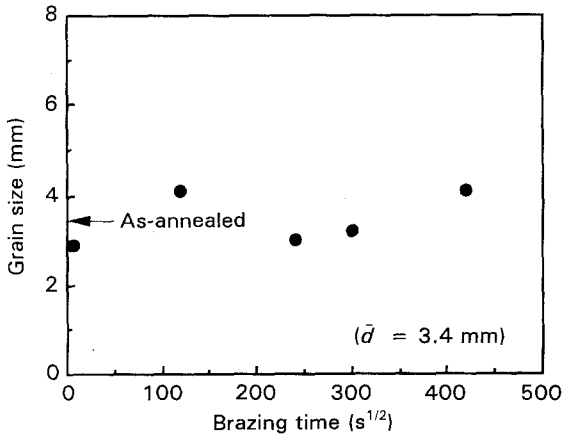

Figure 5 Grain size/holding time relation for coarse-grained nickel base metal.

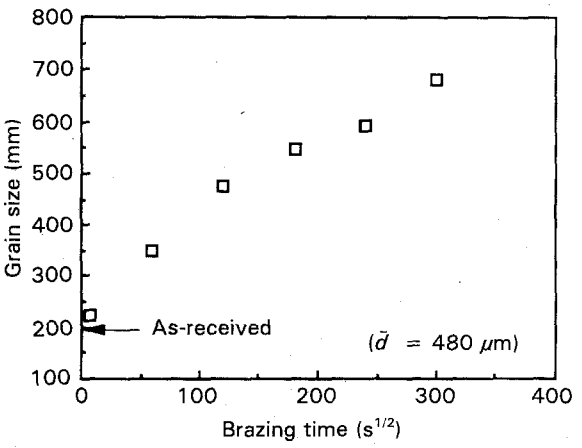

Figure 6 Grain size/holding time relation for fine-grained nickel base metal.

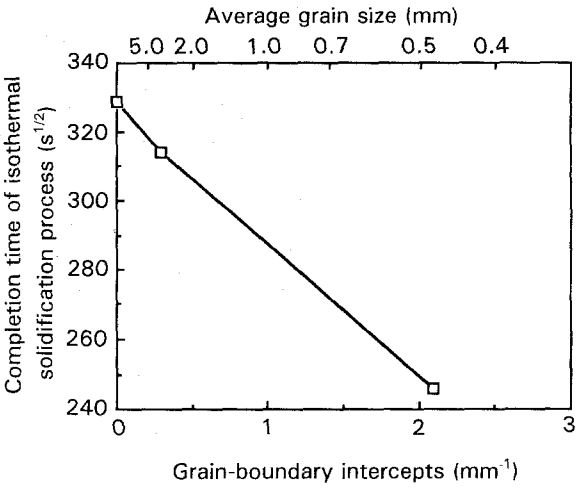

Figure 7 Relation between the completion time for isothermal solidification and the base metal grain size (grain-boundary intercept value); brazing temperature 1150 °C, filler metal thickness 25 μm.

4. Discussion

Fig. 7 shows that there is a direct relation between the mean grain size for the different nickel base metals and the square-root of the completion time during isothermal solidification. In this figure, the grain-boundary intercept value indicates the number of grain-boundary intercepts per unit length in material immediately adjacent to the joint interface (this is the reciprocal of the average grain size of each base metal during isothermal solidification). It is apparent that the completion time for isothermal solidification decreased almost linearly with decrease in the grain size of the nickel base metal.

The relation between the isothermal solidification rate and the base metal grain size is shown in Fig. 8. The isothermal solidification rate in each base metal is the gradient of the relation between the eutectic width and the square-root of brazing time relation (from Fig. 4) and increases when the grain size of the base metal decreases.

It has been suggested that liquid penetration at grain boundaries increases the rate of phosphorus diffusion in solid nickel [9]. However, the effect of grain-boundary regions on movement of the solid–liquid interface during TLP-brazing is extremely complex. For example, the shape of the solid–liquid interface is altered due to liquid penetration, the grain-boundary regions intersect the solid–liquid interface at different angles, base metal grain growth occurs during the brazing process, and so on. Bearing this in mind, a quantitative estimation of the grain-boundary effect is not possible at the present time. Owing to this complexity, a simple qualitative argument which explains the influence of base metal grain boundaries

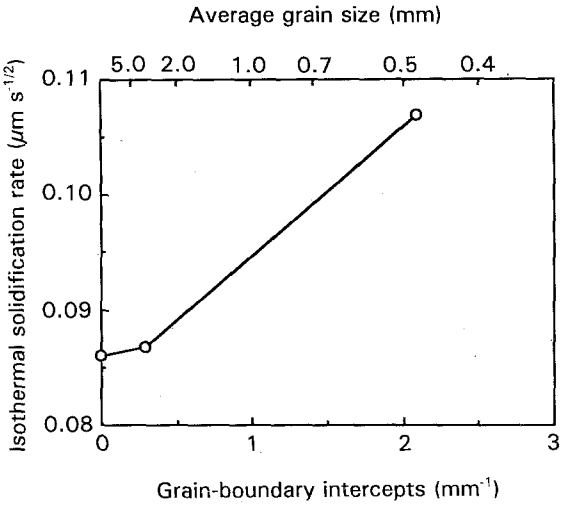

Figure 8 Relation between the rate of isothermal solidification and the base metal grain size (grain-boundary intercept value); brazing temperature 1150 °C, filler metal thickness 25 μm.

will be presented. Using the Ni–P phase diagram (Fig. 9) the liquid width, W_l, at the brazing temperature during isothermal solidification can be expressed as a function of brazing time, t, according to the relation

$$W_l = (OE/OA)\, t_f - [4C_s/(V_s \pi^{1/2})] \times (C_l/V_l - C_s/V_s)^{-1}(D_p t)^{1/2} \quad (1)$$

where t_f is the thickness of the filler metal, C_s the molar ratio of phosphorus in the solid nickel (given by the relation $C_s = 0.810 - 5.565 \times 10^{-4}\, T$, where T is temperature in Celsius [13, 14]; using this relation, C_s is 0.0017 at 1150 °C), C_l is the molar ratio of phosphorus in the liquid phase, (given by the relation $C_l = 48.1 - 0.033\, T$ [13, 14]; using this relation, C_l is 0.1015 at 1150 °C, V_s is the molar volume of solid (6.19 $cm^3\, mol^{-1}$ [15]), V_l the molar volume of liquid (6.68 $cm^3\, mol^{-1}$ [15]), and D_p the diffusion coefficient of phosphorus in solid nickel.

Using Fig. 9, the eutectic width, W_e, during isothermal solidification is related to W_l, namely

$$W_e = W_l[1 + (AE/OA)(\rho_e/\rho_s)]^{-1} \quad (2)$$

where ρ_e is the density of the eutectic phase (7.97 $g\, cm^{-3}$ [15]), and ρ_s the density of the nickel solid solution (8.91 $g\, cm^{-3}$ [15]).

The gradient of the eutectic width/(holding time)$^{1/2}$ relation, m, can be evaluated as follows

$$m = -[1 + (AE/OA)(\rho_e/\rho_s)][4C_s/(V_s \pi^{1/2})] \times (C_l/V_l - C_s/V_s)^{-1} D_p^{1/2} \quad (3)$$

The apparent average diffusion coefficient of phosphorus in solid nickel, D_p, can therefore be back-calculated using Equation 3 and is related to base metal grain size in Fig. 10. Fig. 10 also includes the value found by Nakao *et al.* [15] ($D_p = 1.8 \times 10^{-11}\, m^2\, s^{-1}$) when joining polycrystal nickel, which had been annealed at 1300 °C for 10 min prior to brazing. Although the grain size of the nickel base metal employed in Nakao *et al.*'s study was not documented, it is likely that its grain size fell within the range of the fine-grained and Ohno-cast materials used in the present study. With this in mind, the apparent mean diffusion coefficients of phosphorus found using Ohno-cast and fine-grained nickel are quite consistent with Nakao *et al.*'s result.

It is well-known that solute diffusion at grain-boundary regions is much faster than volume diffusion. Although our results are qualitatively consistent with finer grain size promoting increased solute diffusion into solid nickel, the actual isothermal solidification process is complicated by factors such as liquid penetration at grain boundaries (which increases the surface area available for diffusion at the solid–liquid interface) and base metal grain growth (which may change during the brazing period and modify the influence of grain boundaries on movement of the solid–liquid interface).

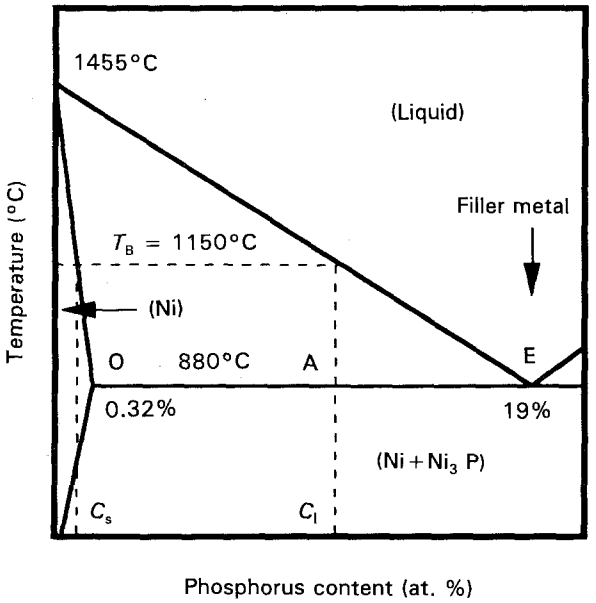

Figure 9 Phase diagram for the Ni–P system.

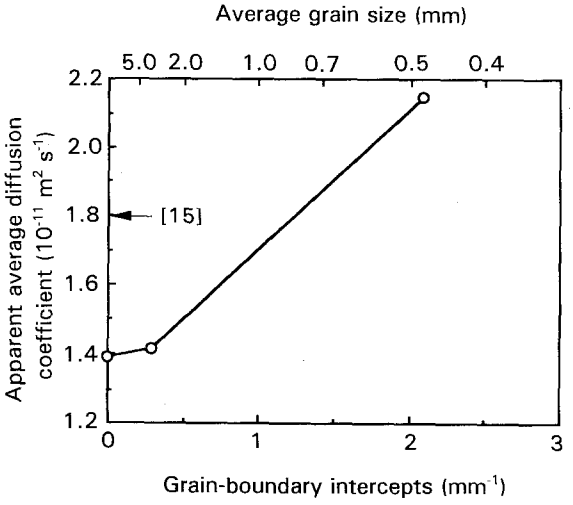

Figure 10 Calculated apparent mean diffusion coefficient values for phosphorus in solid nickel as a function of base metal grain size (grain-boundary intercept value) at 1150 °C.

4. Conclusions

The influence of base metal grain size on the completion time required for isothermal solidification during TLP brazing of nickel using Ni–11 wt % P filler metal was examined. The principal conclusions are summarized as follows.

1. The average eutectic width decreased linearly with the square-root of brazing time in all nickel base metals, and the rate of isothermal solidification increased in the order single-crystal, coarse-grained and fine-grained nickel.

2. The difference in isothermal solidification rates in the different nickel base metals can be qualitatively explained by the effect of grain-boundary regions on the apparent mean diffusion coefficient of phosphorus in solid nickel. The apparent mean diffusion rate of phosphorus in solid nickel increased when the grain size of the nickel decreased.

Acknowledgements

The authors thank the Ontario Center for Materials Research (OCMR) and the Welding Research Council (New York) for financial support of this programme, and also W. Fearis, for his considerable contribution in terms of specimen preparation and brazing experimentation.

References

1. C. IKAWA and Y. NAKAO and T. ISAI, *Trans. Jpn Weld. Soc.* **10** (1979) 24.
2. Y. NAKAO, K. NISHIMOTO, K. SHIMOZAKI and C. KANG, "Transient Liquid Insert Metal Diffusion Bonding of Ni-Base Cast Superalloy MM007", International Institute for Welding, Abingdon, UK, Document No. IA-334-86-OE (1986).
3. W. F. GALE and E. R. WALLACH, *Metall. Trans.* **22A** (1991) 2451.
4. Y. NAKAO, K. NISHIMOTO, K. SHINOZAKI and C. KANG, "Superalloys, 1988", (TMS-AIME, Warrendale, PA, 1989), p. 775.
5. S. LIU, D. L. OLSON, G. P. MARTIN and G. R. EDWARDS, *Weld. J.* **70** (1991) 207s.
6. H. NAKAGAWA, C. H. LEE and T. H. NORTH, *Metall. Trans.* **22A** (1991) 543.
7. T. H. NORTH, K. IKEUCHI, Y. ZHOU and H. KOKAWA, in TMS Symposium, "The Metal Science of Joining", 21st October 1991, edited by M. J. Cieslak, J. H. Perepezko, S. Kang and M. E. Glicksman (TSM, Warrendal, PA), pp. 83–91.
8. I. TUAH-POKU, M. DOLLAR and T. B. MASSALSKI, *ibid.* **19A** (1988) 675.
9. H. KOKAWA, C. H. LEE and T. H. NORTH, *Metall. Trans.* **22A** (1991) 1627.
10. K. IKEUCHI, Y. ZHOU, H. KOKAWA and T. H. NORTH, *ibid.* **23A** (1992) 2905.
11. A. OHNO, in "Proceedings, Metallurgical Processes for the Year 2000 and Beyond", (TMS, Las Vegas, NV, 1989) p. 155.
12. A. OHNO, H. SODA, A. MCLEAN and H. YAMAZAKI, in "Proceedings of the Special Technical Programming Focus on Advanced Materials" (SME, Salt Lake City, UT, 1990), p. 161.
13. T. B. MASSALSKI, "Binary Alloy Phase Diagrams", Vol. 2 (ASM, Metals Park, OH, 1986).
14. P. NASN, "Phase Diagrams of Binary Nickel Alloys" (ASM International, Materials Park, OH, 1991).
15. Y. NAKAO, K. NISHIMOTO, K. SHINOZAKI and C. KANG, *Q. J. Jpn Weld. Soc.* **7** (1989) 213 (in Japanese).

Received 8 May 1992
and accepted 5 March 1993